Engineering Transactions, **66**(3): 281–299, 2018, doi: 10.24423/EngTrans.903.20180928
Polish Academy of Sciences • Institute of Fundamental Technological Research (IPPT PAN)
National Engineering School of Metz (ENIM) • Poznan University of Technology

Research Paper

Contact Between 3D Beams with Deformable Circular Cross-Sections – Numerical Verification

Olga KAWA, Przemysław LITEWKA, Robert STUDZIŃSKI

Institute of Structural Engineering
Poznan University of Technology
Piotrowo 5, 60-965 Poznań, Poland
e-mail: {olga.kawa, przemyslaw.litewka, robert.studzinski}@put.poznan.pl

In this paper a numerical analysis of contact between three-dimensional elastic beams with deformations at the contact zone is carried out. The authors propose a new model of beam-to-beam contact which is the continuation of ideas presented in [6, 7, 10]. The results of beam-to-beam contact analysis are compared with the ones for full 3D problem solved in the Abaqus/enviroment. The aim of the conducted numerical simulations was to select the most appropriate 3D model and to use it as a reference to verify the accuracy of the proposed beam-to-beam contact definition. The verifications were carried out for contact between beams with circular cross-sections. The obtained contact forces and the displacements of beams tips for different beams arrangements and boundary conditions showed a satisfactory correlation.

Key words: contact; beams; finite element method; linearization; deformed cross-section; numerical analysis.

1. Introduction

The main purpose of computational contact mechanics is to provide numerical tools to properly describe physical behaviour of bodies coming in contact. With the development of computer methods in the mid-20th century works began on using the numerical methods in contact analysis. The first papers devoted to the finite element method in the contact analysis with large strains were published by Curnier and Alart [2], Simo and Laursen [13], Wriggers and Miehe [14].

Among many other known publications the monographs by Laursen [9] and Wriggers [15] deserve special attention.

The beam-to-beam contact is a special case of interaction between 3D bodies. The recent years saw a relatively wide interest in this subject. There are several related contributions, e.g.: [3, 4, 8, 10, 11, 15, 17] but still there are many issues

that might be addressed. One of these, that the authors are working on is the question of cross-section deformations at the contact zone.

The authors assumed that the beams which are analysed undergo large displacement, the strains remain small and the beams cross-section are deformed. To include the deformation of the cross-sections the classical analytical result from Hertzian theory of contact between two elastic cylinders is used.

In the earlier publications the authors introduced the deformations at the contact zone by adding the value d to the penetration function [6, 7]. This value d was presented as the change of the radii of beams due to the deformation of the cross-section calculated from Hertzian contact [12]. In the iterative solution procedure in the current step d was calculated using the normal force and the normal gap from the previous step. In this paper an interface physical law resulting from the Hertzian formulation was introduced in the contact definition to replace the penalty parameter used in the approach given in [6] and [7]. Because the physical law for contacting bodies is introduced, the model can be called a *high-precision contact* according to the nomenclature introduced in [16].

The curves representing the beams axes are defined using Hermite's polynomials proposed by Litewka [10]. The appropriate kinematic variables for contact were discretised using the finite element method methodology. The beams were modelled using elastic co-rotational finite elements proposed by Crisfield [1].

The results of this approach are compared to the full 3D analysis carried out in Abaqus/CAE with the elastic material assumed. The calculations were performed using the Newton-Raphson procedure. The choice of the appropriate FE model in Abaqus/CAE involved the following aspects: the beams arrangement, the mesh size and the type of finite element. For the comparison of beam-to-beam and full 3D models three verification criteria were considered – the magnitude of the contact forces, macroscopic displacements of beams tips and the size of the deformations of the beams cross-section in the vicinity of the contact points.

2. Beam to beam contact

2.1. Kinematic relations

Two beams with circular cross-sections coming into contact are considered (Fig. 1). The penetration function is written as:

$$g_N = d_n - r_m - r_s, \tag{2.1}$$

where d_n is the minimum distance between axes of the beams, r_m, r_s are radii of the beam cross-sections (Fig. 2).

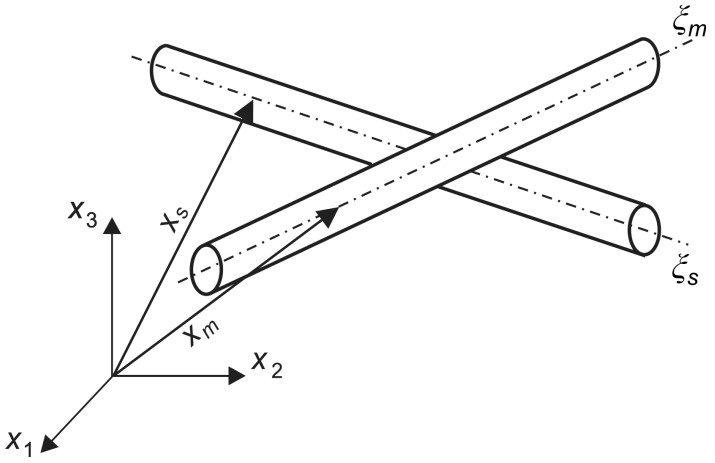

FIG. 1. Contacting beams.

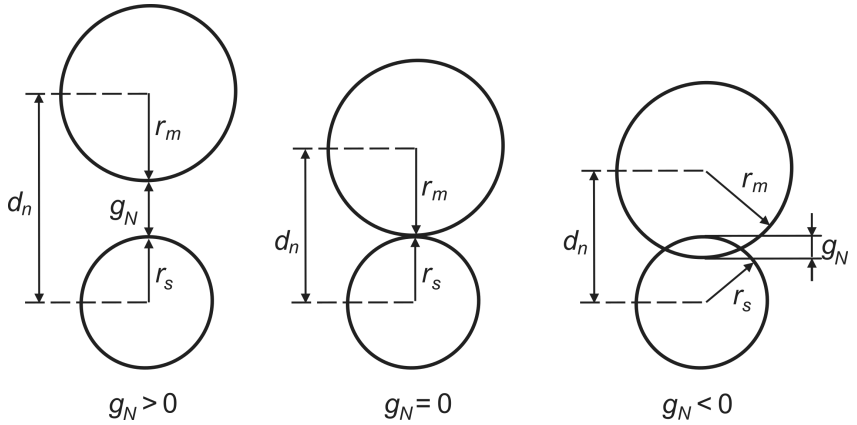

FIG. 2. Contact criterion for beams.

The function of penetration constitutes the criterion of contact (Fig. 2). The contact condition is defined as in [15]:

$$g_N = d_n - r_m - r_s \leq 0. \tag{2.2}$$

To evaluate g_N, the position vectors $\mathbf{x}_{mn}$ and $\mathbf{x}_{sn}$ of two closest points (C_{mn} and C_{sn}) lying on two curves representing the beams axes (m and s) have to be found.

2.2. Contact points

The local curvilinear co-ordinates (ξ_m for first beam, ξ_s for the second one) define the location of the closest points C_{mn} and C_{sn} on the curves in the 3D

space (see Fig. 3). The positions of these points are found on the curves representing beam axes m and s. In the global Cartesian system each point on the curve is associated with a position vector $\mathbf{x}_m$, $\mathbf{x}_s$ The current beams configurations are expressed as:

$$\begin{aligned} \mathbf{x}_m &= \mathbf{X}_m + \mathbf{u}_m, \\ \mathbf{x}_s &= \mathbf{X}_s + \mathbf{u}_s, \end{aligned} \tag{2.3}$$

where $\mathbf{X}_m$, $\mathbf{X}_s$ are the position of vectors at the initial configuration, and $\mathbf{u}_m$, $\mathbf{u}_s$ are the displacement vectors.

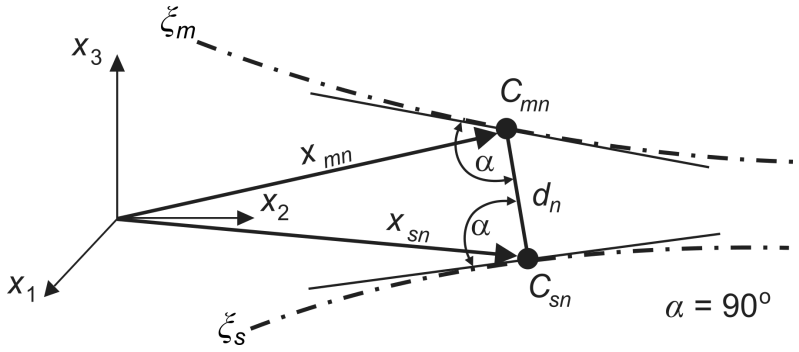

FIG. 3. The closest points on two curves.

The position vectors $\mathbf{x}_{mn}$ and $\mathbf{x}_{sn}$ of the closest points fulfil the orthogonality conditions:

$$\begin{cases} (\mathbf{x}_{mn} - \mathbf{x}_{sn}) \circ \mathbf{x}_{mn,m} = 0, \\ (\mathbf{x}_{mn} - \mathbf{x}_{sn}) \circ \mathbf{x}_{sn,s} = 0, \end{cases} \tag{2.4}$$

where

$$\mathbf{x}_{mn,m} = \frac{\partial \mathbf{x}_{mn}}{\partial \xi_m}, \qquad \mathbf{x}_{sn,s} = \frac{\partial \mathbf{x}_{sn}}{\partial \xi_s}. \tag{2.5}$$

The Newton-Raphson method is used to obtain the solution which defines the location of the points C_{mn} and C_{sn}. The linearization of (2.4) leads to a set of two equations, which allow for calculation of co-ordinate increments $\Delta\xi_s$ and $\Delta\xi_m$. All the quantities involved have to be determined for the current values of the co-ordinates ξ_m and ξ_s [6]. Knowing the position vectors $\mathbf{x}_{mn}$ and $\mathbf{x}_{sn}$ the minimum distance between the beams can be calculated:

$$d_n = \|\mathbf{x}_{mn} - \mathbf{x}_{sn}\|. \tag{2.6}$$

2.3. Hertzian contact

The deformation at the contact zone is included using the classical analytical result from Hertzian contact [5, 12]. The starting point is the case of a rigid sphere contacting with an elastic half-space. The problem of two cylinders with perpendicular axes leads to the same result as for a pair of spheres with radii r_s and r_m [5].

The normal force in the contact zone is defined by:

$$F = \frac{4}{3} \cdot E \cdot R^{1/2} \cdot d^{3/2}, \tag{2.7}$$

where R is value of the effective radius, E is the mean Young's modulus and d is the change of r_m and r_s due to the deformation of cross-sections (Fig. 4).

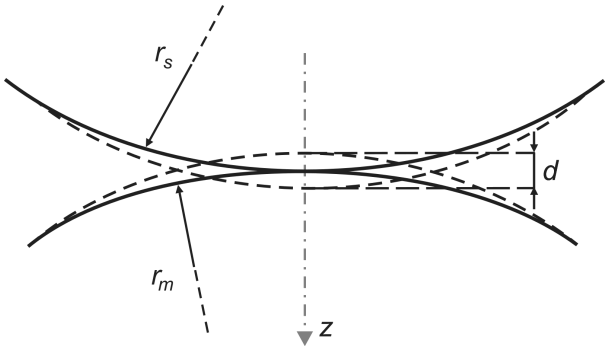

FIG. 4. The contraction of radii of contacting spheres.

In the case of two elastic bodies made of different materials the mean Young's modulus E is used:

$$\frac{1}{E} = \frac{1 - v_s^2}{E_s} + \frac{1 - v_m^2}{E_m}, \tag{2.8}$$

where E_s, E_m are the moduli of elasticity, v_s, v_m are the Poisson's ratios.

In case of two spheres with radii r_s and r_m the value of R is calculated as [12]:

$$\frac{1}{R} = \frac{1}{r_s} + \frac{1}{r_m}. \tag{2.9}$$

In case two crossed cylinders in contact the effective *Gaussian radius* can be used in place R in Hertzian relationships [12].

The contact zone between two cylinders has an elliptic shape with semi-axes:

$$a = (r_s \cdot d)^{1/2} \qquad \text{and} \qquad b = (r_m \cdot d)^{1/2}. \tag{2.10}$$

The contact area is calculated as:

$$A = \pi \cdot d \cdot \widetilde{R}, \tag{2.11}$$

where the effective *Gaussian radius* of curvature of the surface is written as:

$$\widetilde{R} = (r_s \cdot r_m)^{1/2}. \tag{2.12}$$

In our case of contact between beams with perpendicular axes the value of *Gaussian radius* has been used in all calculations.

The value of d in Eq (2.7) can be written as

$$d = \sqrt[3]{\frac{9}{16}} \cdot \frac{F_N^{2/3}}{E^{2/3} \cdot R^{1/3}}. \tag{2.13}$$

In this approach the normal gap used to define contact is assumed as the simple measure of cross-sections deformation, thus:

$$g_N = d, \tag{2.14}$$

so the normal force can be expressed as:

$$F_N = \frac{4}{3} \cdot E \cdot R^{1/2} \cdot g_N^{3/2}. \tag{2.15}$$

Thus, the penalty parameter which is used in the standard penalty method to calculate the normal force:

$$F_N = \varepsilon_N \cdot g_N \tag{2.16}$$

is now replaced by:

$$\varepsilon_N = \frac{4}{3} \cdot E \cdot R^{1/2} \cdot g_N^{1/2}. \tag{2.17}$$

Therefore, in this approach the cross-sections deformation is introduced by replacing the penalty parameter with the Hertzian contact stiffness. It is emphasized, that the main idea was to use such a simple approach without any complex formulations, meant to improve the beam-to-beam contact formulation, which itself is also a simplification of the full 3D analysis.

In the iterative solution procedure in the current step the radii change d is evaluated using the normal force and the normal gap g_N from the current step.

2.4. Weak form and its linearization

For two bodies the solution of contact problem involves finding a minimum of the potential energy functional Π what can be written down as:

$$\min \Pi = \min (\Pi_1 + \Pi_2 + \Pi_c), \tag{2.18}$$

where Π_1, Π_2 are the components of potential energy for the first and the second body, while Π_c is the part of the energy related to contact. This leads to a solution of a functional minimization with inequality constraints. Using the concept of an active set the inequality constraints can be replaced by the equality constraints [10].

The contact contribution to the corresponding weak form is [16]:

$$\delta \Pi_c = F_N \delta g_N. \tag{2.19}$$

Substituting from Eq. (2.12) gives:

$$\delta \Pi_c = \frac{4}{3} \cdot E \cdot R^{1/2} \cdot g_N^{3/2} \delta g_N. \tag{2.20}$$

The linearization required for the Newton solution scheme for the non-linear contact problem is written as:

$$\Delta \delta \Pi_c = \left(2 \cdot E \cdot R^{1/2} \cdot g_N^{1/2}\right) \Delta g_N \delta g_N + \left(\frac{4}{3} \cdot E \cdot R^{1/2} \cdot g_N^{3/2}\right) \Delta \delta g_N. \tag{2.21}$$

The variation, linearization and second variation of the penetration function g_N are obtained just like in the case without the cross-section deformation – they are presented in detail in [10].

3. Finite element model definition in Abaqus/CAE

The aim of the conducted numerical simulations in the Abaqus/CAE program was a verification of the developed beam-to-beam contact model, which is able to describe the contact interface between beams of circular cross-section. It is well known that the finite element simulations are very sensitive to both the type of the finite element and the mesh size. Therefore, the convergence analysis of the finite element model was performed first.

Numerical data for all the calculations here and for all the examples in Sec. 4 are given without any specified physical units, though it is understood, that any consistent unit set might be used.

The analytical solutions of the clamped-clamped beam with concentrated force applied at the mid-span were used as reference solutions (Fig. 5). The

beam of the length 2000 and circular cross-section with the diameter 100 was assumed. The linear elastic material with data matching polypropylene was implemented. Therefore, the following parameters were assumed: Young modulus $E = 2500$, Poisson ratio $\nu = 0.4$. The geometrical and material characteristics of the reference beam fulfil the assumptions of the Euler-Bernoulli thin beam theory.

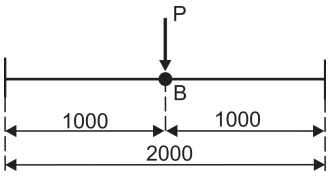

FIG. 5. The initial configuration of beam axes for verification procedure.

The convergence analysis of the numerical model comprises not only the mesh size and the shape of a finite element but also the type of shape function, number of nodes, and number of integration points, see Table 1. All calculations were performed using the Newton-Raphson procedure.

Table 1. The set of the parameters used in convergence analysis.

No.	Name of the FE	Type of the FE	Shape function of the FE	No. of nodes	Reduced integration	Mesh size
1	C3D8	brick	linear	8	no	25 / 20 / 10 / 5
2	C3D8R		linear	8	yes	25 / 20 / 10 / 5
3	C3D20		quadratic	20	no	25 / 20 / 10
4	C3D20R		quadratic	20	yes	25 / 20 / 10
5	C3D4	tetrahedron	linear	4	no	25 / 20 / 10 / 5
6	C3D10		quadratic	10	no	20 / 20 / 10

The three verification criteria were considered: the magnitude of displacement at the point Bu_B, the normal stresses due to bending at the point B σ_B, and CPU time of the analysis. The results of the convergence analysis are presented in the graph in Figs. 6a–6c.

According to the performed analyses the following conclusions can be formulated. All the finite elements, if they are small enough, correctly predict the analitycally obtained displacement. Nevertheless, the results should not be too sensitivite to the mesh size. Thus, the tetrahedron element C3D4 and brick elements C3D8, C3D8R do not fullfill the above mentioned requirement. Please note that these elements have linear shape functions. On the contrary the finite elements with quadratic shape functions (tetrahedron C3D10 and brick C3D20,

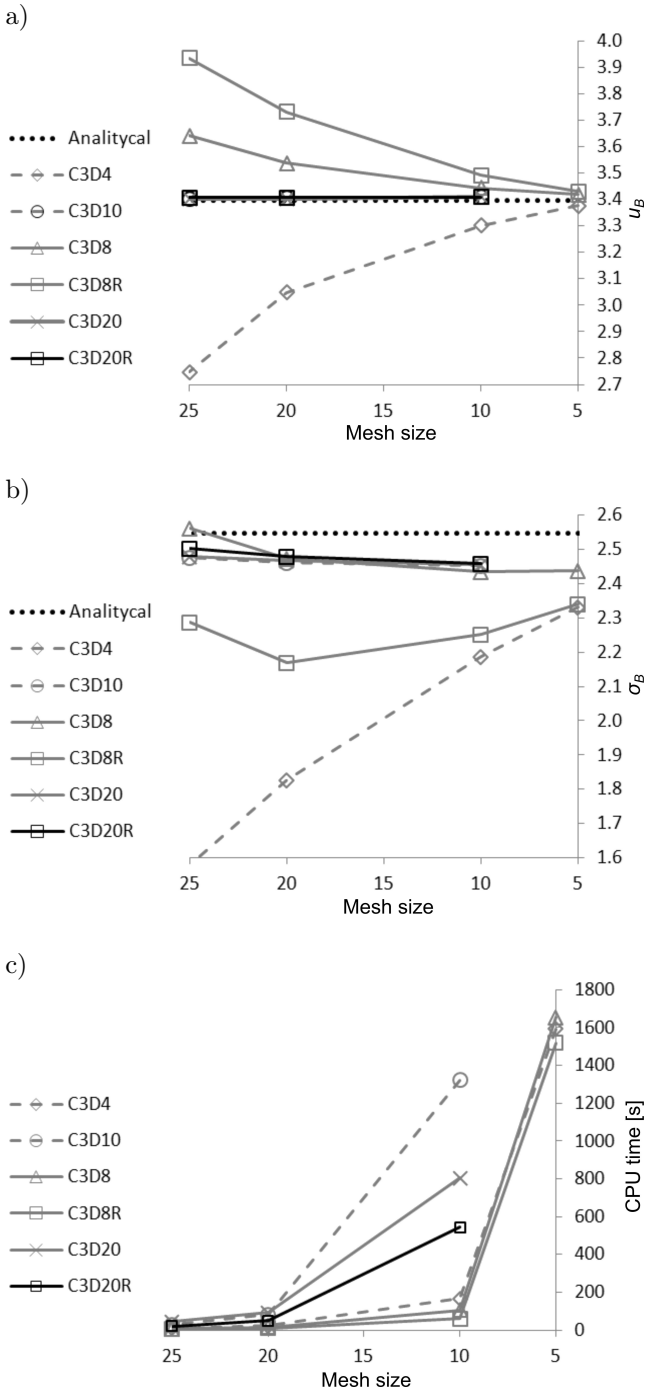

FIG. 6. Results of the convergence analysis: a) displacement of the midpoint u_B, b) normal bending stresses in the middle cross section σ_B, c) CPU time.

C3D20R) are not so much sensitive to the mesh size. A similar observation applies to the normal stress criterion (stress at the point B, σ_B). Finally, taking into account the third criterion – computational cost (CPU time criterion), the C3D20R finite element with 10 mesh size will be used for further analyses.

4. Numerical examples

4.1. Introduction

Three examples of beam-to-beam contact are presented in this section. It is assumed that the beams which are analysed undergo large displacements, the strains remain small and the beams cross-sections are deformed.

In the beam-to-beam model each beam is discretized using twenty finite elements proposed by Crisfield [1]. The Hermite's polynomials used by Litewka [10] are representing the curves of the beams. The imposed displacements are applied simultaneously in 60 or 30 equal increments.

In the 3D finite element simulations in Abaqus/CAE the 20-node quadratic brick (C3D20R) finite elements were used, as was decided in Sec. 3.

4.2. Example 1

In this example contact between two clamped-clamped beams is considered. The beams have circular cross-sections with radius $r = 0.1$, length 6.0 and are initially spaced at 0.001. They are made of a material with Young's modulus $E = 210 \cdot 10^9$ and Poisson's ratio $v = 0.3$. The imposed displacements $\Delta = 0.1$ are shown in Fig. 7.

Different positions of the axis of the second beam are analyzed. Nine cases of the location of the beam axis are considered, separated by 0.3 intervals. The initial configuration of beams axes is shown in Fig. 7.

The values of the normal contact forces obtained from beam-to-beam contact results and Abaqus/CAE are presented in Table 2. In Table 3 the values of the deformations of the cross-sections are shown The deformed configuration of beams axes for the case when $\delta = 1.5$ is presented in Fig. 8.

The forces in contact are in a good agreement nevertheless in the case of the measured deformation the differences are observed. Please note that in Abaqus/CAE the direct (Lagrange multipliers) constraint enforcement method is applied. The symmetrical arrangement of the beams ($\delta = 0$) leads to the measured deformations of the same order however for non-symmetrical arrangements of the beams ($\delta \geq 0$) the differences in measured deformations made them incomparable. This is due to the way of the definition of control points in Abaqus/CAE. The control points are arbitrarily defined for an undeformed structure, therefore in the case of the non-symmetrical beams arrangement these

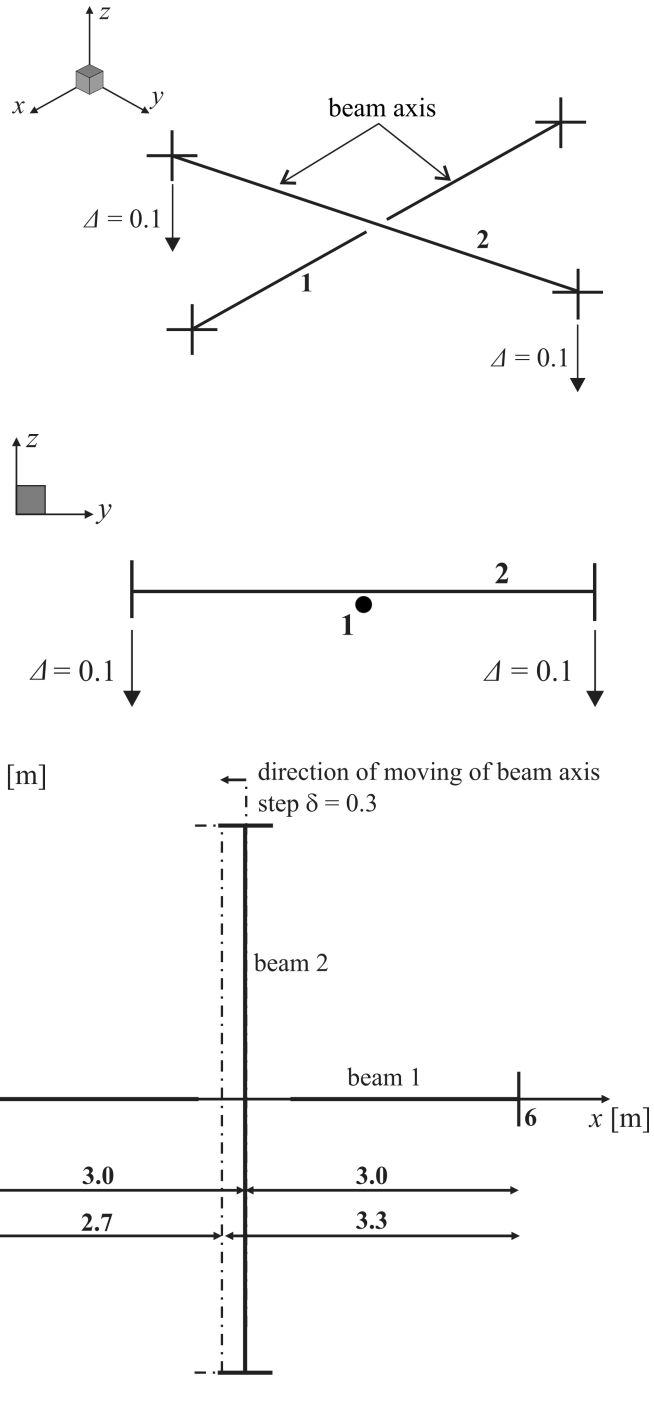

FIG. 7. The initial configuration of beam axes in Example 1.

Table 2. Values of the normal forces in Example 1.

Position of the second beam δ	Beam-to-beam contact	Abaqus/CAE	Difference [%]
0.0	773266.24190	760881.0	1.92
0.3	790569.97470	772169.0	2.33
0.6	827762.21950	818256.0	1.15
0.9	892470.60020	881160.0	1.27
1.2	990058.97810	975741.0	1.45
1.5	1124437.50829	1106910.0	1.56
1.8	1297977.33058	1276190.0	1.68
2.1	1499411.40150	1471200.0	1.88
2.4	1683555.62630	1651970.0	1.88
2.7	1781586.32080	1758500.0	1.30

Table 3. Values of the deformation of the cross-section in Example 1 for the symmetrical arrangement of the beams.

Position of the second beam δ	Beam-to-beam contact	Abaqus/CAE	Difference [%]
0.0	0.000632	0.000616	2.59

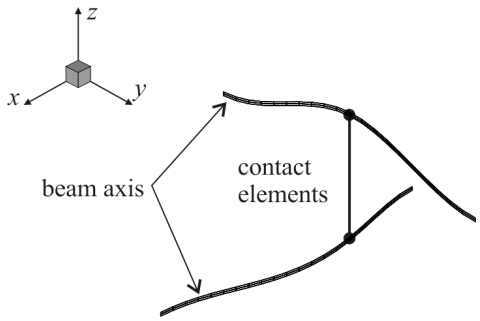

FIG. 8. Deformed configuration of beam axes for $\delta = 1.5$ in Example 1.

points do not coincide precisely with the real contact points. It generates the false values of the deformation.

In the Abaqus/CAE analysis the deformation δ is calculated as the difference between the displacements of the control points for undeformed and deformed configurations of beams (see Fig. 9):

$$u'_{AB} + u_A + r = 2r + gap + r + u_B,$$
$$\delta = 2r - u'_{AB}. \tag{4.1}$$

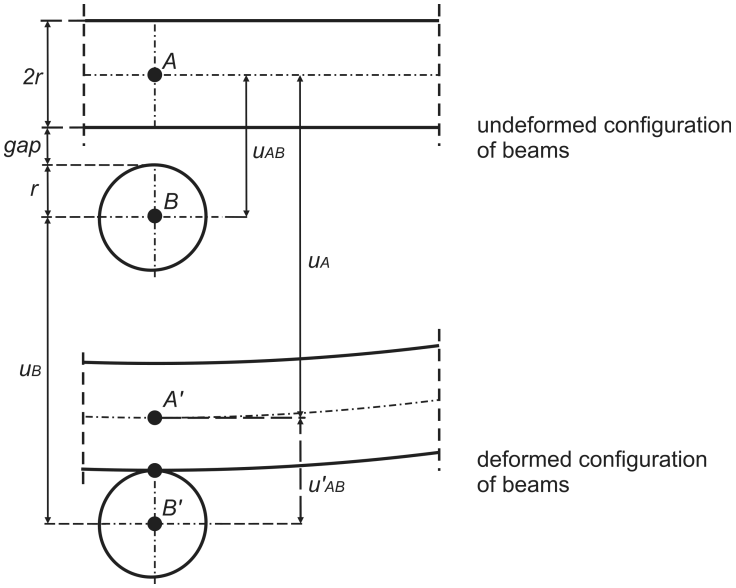

FIG. 9. Location of the control points for undeformed and deformed beams.

For the symmetrical arrangement of the beams the authors calculated the normal force and the value of the deformation of the cross-section for another set of values for Young's modulus and Poisson's ratio: $E = 250 \cdot 10^7$, $\nu = 0.4$. The results are presented in the Table 4. As previously, the normal force and the deformation of the cross-section are in a good agreement.

Table 4. Values of the normal force and the deformation of the cross-section in Example 1 for another set of values of $E = 250 \cdot 10^7$, $\nu = 0.4$.

	Beam-to-beam contact	Abaqus/CAE	Difference [%]
Normal forces	9208.94	9068.36	1.55
Deformation of the cross-section	0.0005995	0.0005542	8.17

4.3. Example 2

Contact between two cantilever beams is considered. The initial configuration of beam axes is shown in Fig. 10. The beams have circular cross-sections with radius $r = 0.1$, length 6.0 and are initially spaced at 0.001. They are made of a material with Young's modulus $E = 210 \cdot 10^5$ and Poisson's ratio $v = 0.3$. The imposed displacements are shown in Fig. 10. They are applied simultaneously in 60 equal increments. Thirteen different cases of beams layout are considered with 0.3 interval between the beams axes location.

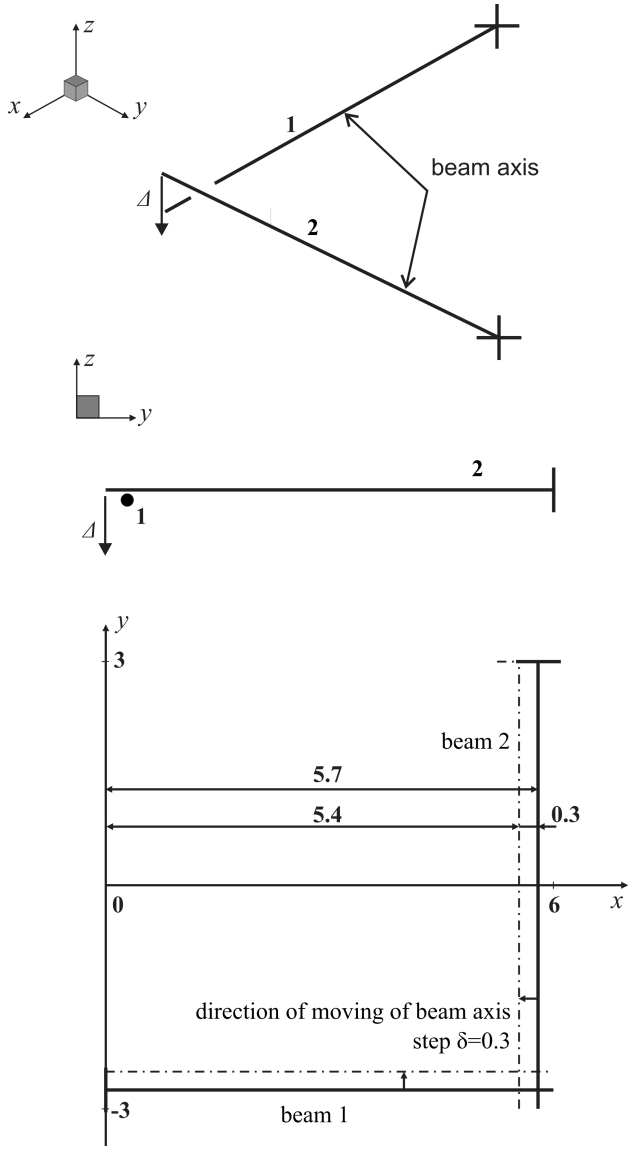

FIG. 10. The initial configuration of beams axes in Example 2.

Table 5 includes the values of the normal forces at the contact zone. Additionally, for this example the values of displacements of beams tips for three selected cases are presented in Table 6. The deformed configuration of beams axes is presented in Fig. 11.

It can be seen, that the calculated displacements of beam tips remain in a good coincidence between two compared calculation methods. The difference

Table 5. Values of the normal forces in Example 2.

Position of the second beam x	Beam-to-beam contact	Abaqus/CAE	Difference [%]
1.8	5.898687649	5.63627000	4.45
2.1	5.340425604	5.14890000	3.59
2.4	4.883922954	4.72851000	3.18
2.7	5.030142717	4.88361000	2.91
3	4.659135383	4.52692000	2.84
3.3	4.329716083	4.22213000	2.48
3.6	4.027222964	3.93403000	2.31
3.9	3.372044968	3.29694000	2.23
4.2	3.132804306	3.08498000	1.53
4.5	2.594303241	2.55779000	1.41
4.8	2.117062089	2.08630000	1.45
5.1	1.693392608	1.66470000	1.69
5.4	1.316320841	1.28851000	2.11

Table 6. Values of displacements of the ends of the beams in Example 2.

Position of the second beam x	Beam-to-beam contact		Abaqus/CAE		Difference [%]	
	Beam 1	Beam 2	Beam 1	Beam 2	Beam 1	Beam 2
1.8	−0.03122254	−0.09	−0.0297660	−0.09	4.89	0
3.0	−0.06239676	−0.10	−0.6169660	−0.10	1.13	0
4.5	−0.07098216	−0.08	−0.0704139	−0.08	0.81	0

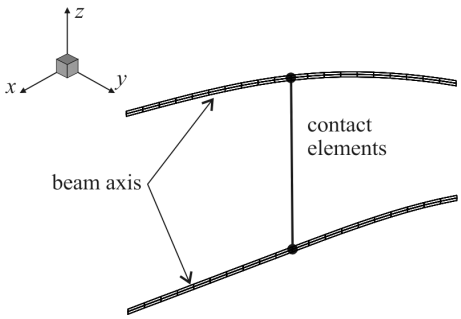

FIG. 11. Deformed configuration of beam axes for $\delta = 3.0$ in Example 2.

does not exceed several percent – it is 4.9% for the most extreme case. Due to the non-symetric arrangement of the beams the magnitude of the deformation is not compared.

4.4. Example 3

In this example contact between four beams is analyzed (Fig. 12). The beams have circular cross-sections with radius $r = 0.1$, length 8.0 and are made of the material with $E = 250 \cdot 10^7$ and $v = 0.3$. The ends of beams are subjected to displacements $\Delta = 0.5$ applied in 30 equal increments. Each of the beams has almost fully constrained centre points, except for the freedom of rotation about the axes lying in the plane perpendicular to the beams (see Fig. 12).

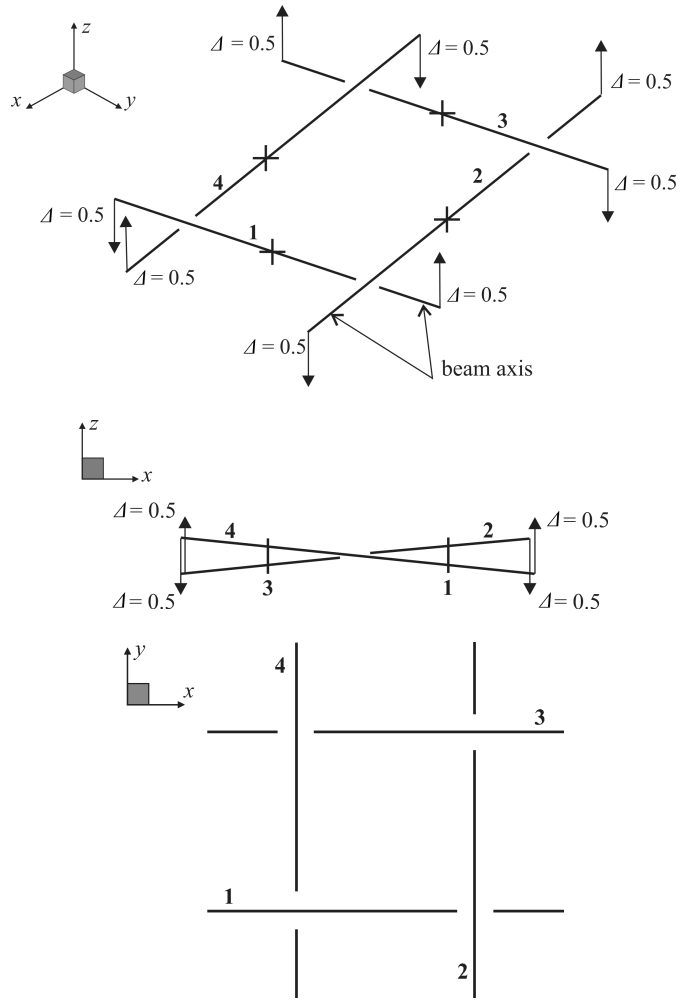

Fig. 12. The initial configuration of beams axes in Example 3.

The results of analysis: values of the normal forces are presented in Table 7. Deformed configuration of beams axes is presented in Fig. 13. Figure 14 shows the view of deformed beams.

Table 7. Values of the normal forces in Example 3.

	Beam-to-beam contact	Abaqus/CAE	Difference [%]
Normal forces	28820.0	26369.0	8.5

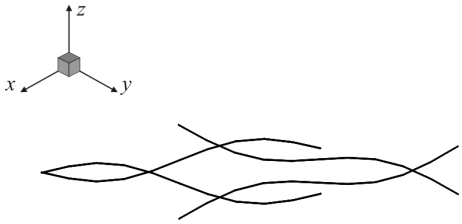

Fig. 13. Deformed configuration of beams axes in Example 3.

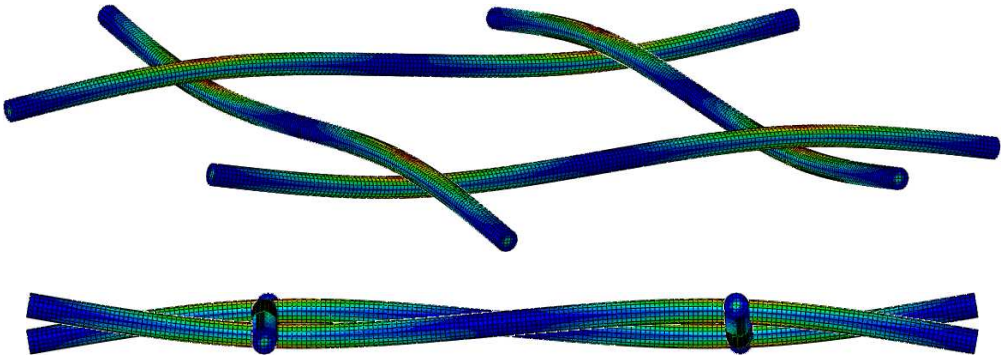

Fig. 14. View of deformed beams in Example 3.

As in previous examples the forces in contact are in a good agreement, while the magnitude of the deformation is not compared due to the non-symetric arrangement of the beams.

5. Summary

In this paper the verification of the new beam-to-beam contact approach has been presented. This approach allows for a simple means of inclusion of the cross-section deformation of the beams in contact. The verification was carried out using numerical simulations in the Abaqus/CAE. Three verification criteria were considered, the first one was the magnitude of the contact force, the second one – the size of the deformations of the beams cross-section in the vicinity of the contact points and the third one – the beams tips displacements.

The presented results indicate that the type of the finite element in Abaqus/CAE has qualitative and quantitative influence on the numerical results. The

most accurate finite element was used for the verification procedure. The obtained contact forces and the displacements of the ends of the beams for different beams arrangements (symmetrical and asymmetrical) and beam boundary conditions showed a satisfactory correlation (differences smaller then several percent) between the considered models.

The deformation of beams cross-sections cannot be compared effectively when the non-symetrical arrangements of the beams is assumed. Only for the case of the symmetrical arrangement of the beams (see Example 1, $\delta = 0$) the values of the deformations of the cross-section calculated using Abaqus/CAE correspond to the beam-to-beam solution. In the presented beam-to-beam model the physical law for contacting bodies is introduced, so the gap function is the real value of the deformation of the cross-sections free of any geometric inaccuracy.

Finally, it can be stated that the proposed beam-to-beam contact model is an attractive, yet simple method of analysis for contacting beams, leading to relatively accurate results obtained with a much smaller computational cost – the analyses in Abaqus/CAE took a significantly longer time (hundreds of times longer).

References

1. Crisfield M.A., *A consistent co-rotational formulation for non-linear, three-dimensional beam-elements*, Computer Methods in Applied Mechanics and Engineering, **81**(2): 131–150, 1990.
2. Curnier A., Alart P., *A generalized Newton method for contact problem with friction*, Journal de Mécanique Théorique et Appliquée, **7**: 67–82, 1988.
3. Durville D., *Contact-friction modeling within elastic beam assemblies: An application to knot tightening*, Computational Mechanics, **49**(6): 687–707, 2012.
4. Gay Neto A., Pimenta P.M., Wriggers P., *Self-contact modeling on beams experiencing loop formation*, Computational Mechanics, **55**(1): 193–208, 2015.
5. Johnson K.L., *Contact mechanics*, pp. 81–104, Cambridge University Press, 1985.
6. Kawa O., Litewka P., *Contact between 3-D beams with deformable circular cross sections*, [in:] *Recent Advances in Computational Mechanics*, T. Łodygowski, J. Rakowski, P. Litewka (Eds.), pp. 183–190, CRC Press/Balkema, Taylor & Francis Group, London, 2014.
7. Kawa O., Litewka P., *Contact with friction between 3D beams with deformable circular cross sections*, Engineering Transactions, **63**(4): 439–462, 2015.
8. Konyukhov A., Schweizerhof K., *Geometrically exact theory for arbitrary shaped bodies*, Lecture Notes in Applied and Computational Mechanics, Vol. 67, Springer, 2013.
9. Laursen T.A., *Computational contact and impact mechanics*, Springer, Heidelberg, 2002.
10. Litewka P., *Finite element analysis of beam to beam contact*, Springer, Berlin–Heidelberg, 2010.

11. Meier C., Wall W., Popp A., *A unified approach for beam-to-beam contact*, Computer Methods in Applied Mechanics and Engineering, **315**: 972–1010, 2017.

12. Popov V.L., *Contact Mechanics and Friction*, pp. 55–64, Springer, Berlin–Heidelberg, 2010.

13. Simo J.C., Laursen T.A., *An augmented Lagrangian treatment of contact problems involving friction*, Computers and Structures, **42**(1): 97–116, 1992.

14. Wriggers P., Miehe C., *On the treatment of contact contraints within coupled thermomechanical analysis*, [in:] *Proceedings of EUROMECH, Finite Inelastic Deformations*, Desdo B., Stein E. (Eds.), Springer, Berlin 1992.

15. Wriggers P., Zavarise G., *On contact between three-dimensional beams undergoing large deflections*, Communications in Numerical Method in Engineering, **13**(6): 429–438, 1997.

16. Wriggers P., *Computational contact mechanics*, 1st Ed., pp. 339–354, Wiley, 2002.

17. Zavarise G., Wriggers P., *Contact with friction between beams in 3-D space*, International Journal for Numerical Methods in Engineering, **49**(8): 977–1006, 2000.

Received April 10, 2018; accepted version May 28, 2018.